Supplementary information

All-Optically Modulated PDVT-10/IGZO Heterojunction Synapses for Neuromorphic Applications

Shanshan Jiang[a], Kesheng Wang[a], Yujiao Li[b], Jiawei Yang[b], Bingyan Wang[b], Peng Chen[b], Bo He[b], Huanhuan Wei[b], Changjin Wan[c*], and Gang He[b*]

S. S. Jiang, K. S. Wang
School of Integrated Circuits, Anhui University, Hefei 230601, China
Y. J. Li, J. W. Yang, B. Y. Wang, P. Chen, B. He, H. H. Wei, G. He
School of Materials Science and Engineering, Anhui University, Hefei, 230601, P.R. China
E-mail: hegang@ahu.edu.cn
C. J. Wan
School of Electronic Science & Engineering, Nanjing University, Nanjing 210093, China.
E-mail: cjwan@nju.edu.cn

Supplementary Figures：

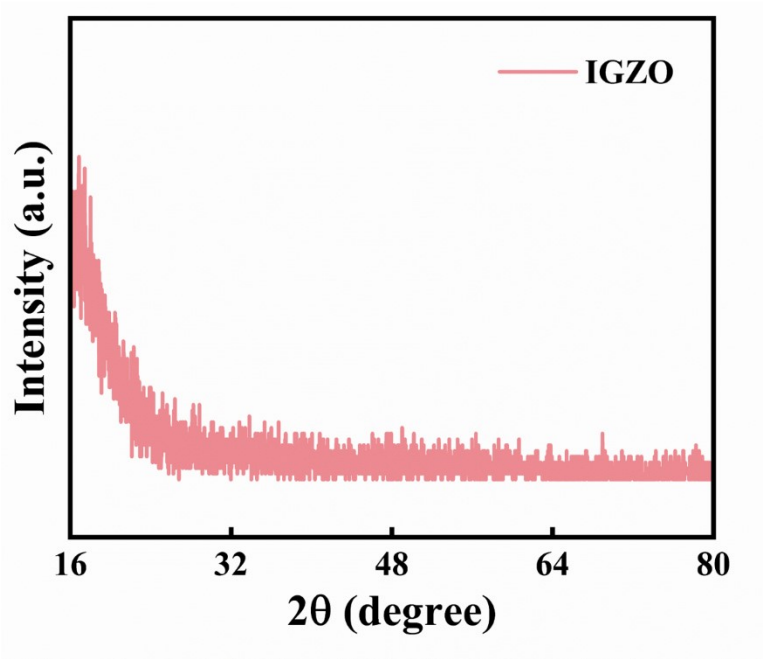

Fig. S1 XRD spectrum of amorphous IGZO.

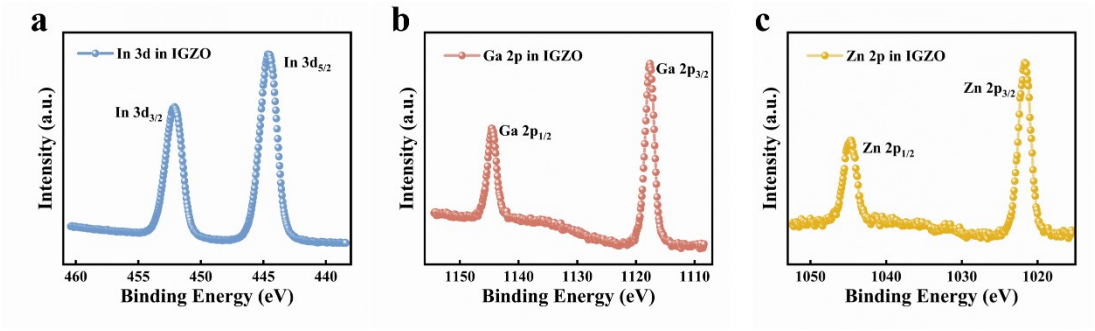

Fig. S2 (a) XPS spectrum of In 3d in IGZO; (b) that of Ga 2p; (c) that of Zn 2p.

Binding energy calibration was performed using the C 1s signal at 284.8 eV as the reference. The peaks corresponding to In $3d_{5/2}$, Ga $2p_{3/2}$ and Zn $2p_{3/2}$ are located in 444.6 eV, 1117.6 eV and 1021.7 eV, which are corresponding to In-O band, Ga-O bond, and Zn-O bond, respectively.[1,2]

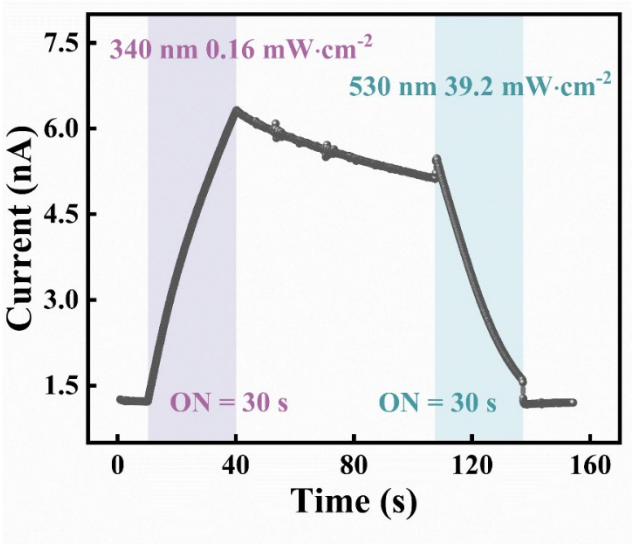

Fig. S3 Reversible photocurrent modulation induced by 340 nm (0.16 mW·cm^{-2}, 30 s) and 530 nm (39.2 mW·cm^{-2}, 30 s) light.

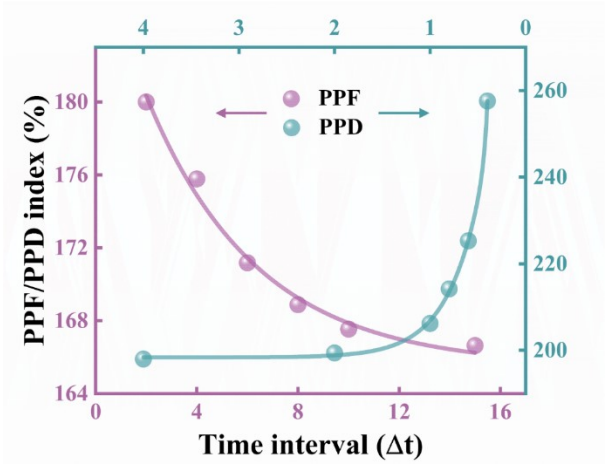

Fig. S4 PPF/PPD index plotted as a function of the time interval (Δt).

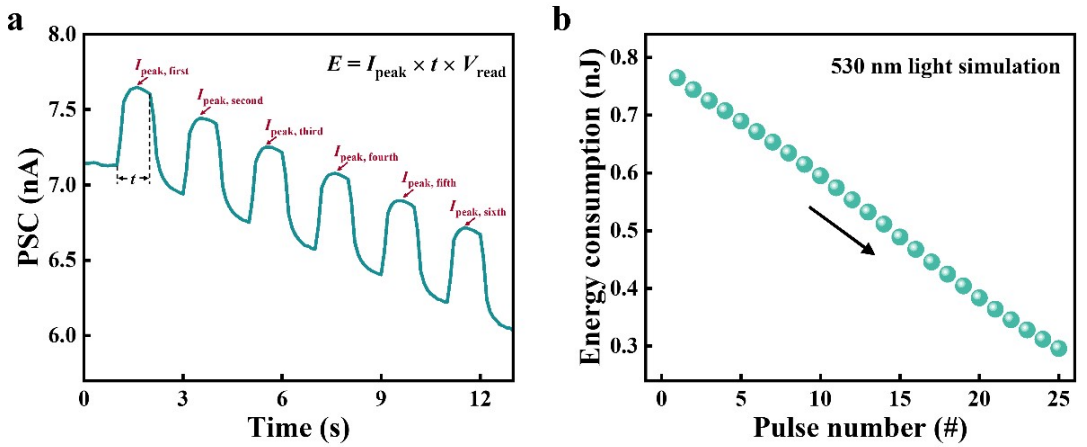

Fig. S5 Calculation of energy consumption. (a) PSC response to 530 nm (39.2 mW·cm^{-2}) light pulses, with I_{peak} extracted for energy consumption calculation. (b) Energy consumption per light pulse as a function of pulse number.

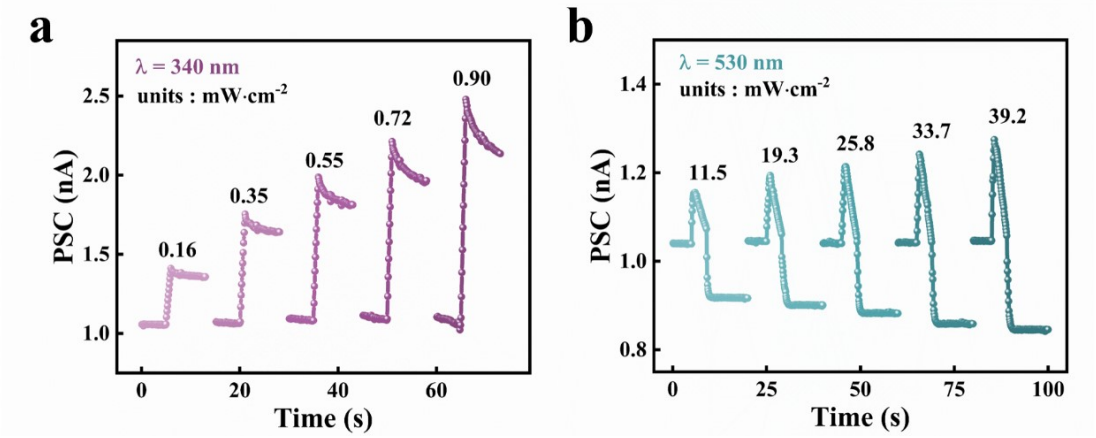

Fig. S6 Bidirectional light intensity-dependent plasticity under (a) 340 nm and (b) 530 nm light pulse, respectively.

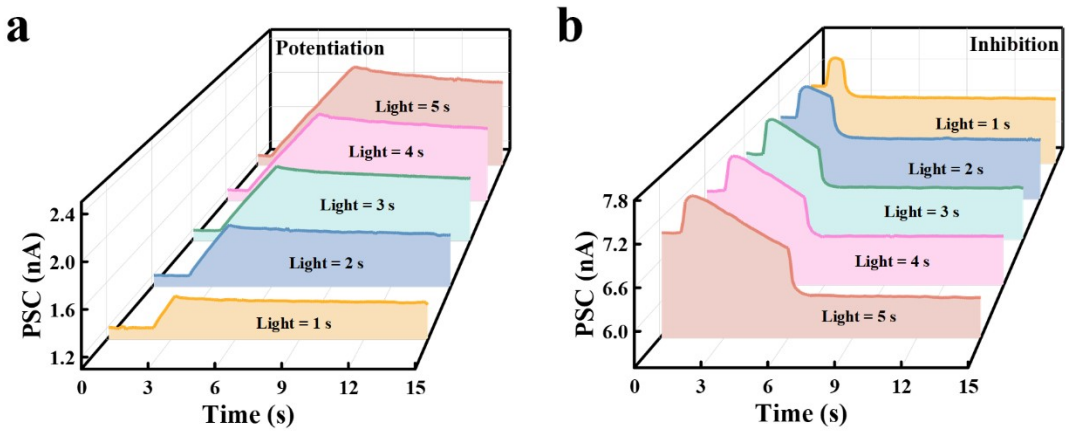

Fig. S7 Bidirectional light duration-dependent plasticity under (a) 340 nm and (b) 530 nm light pulse, respectively.

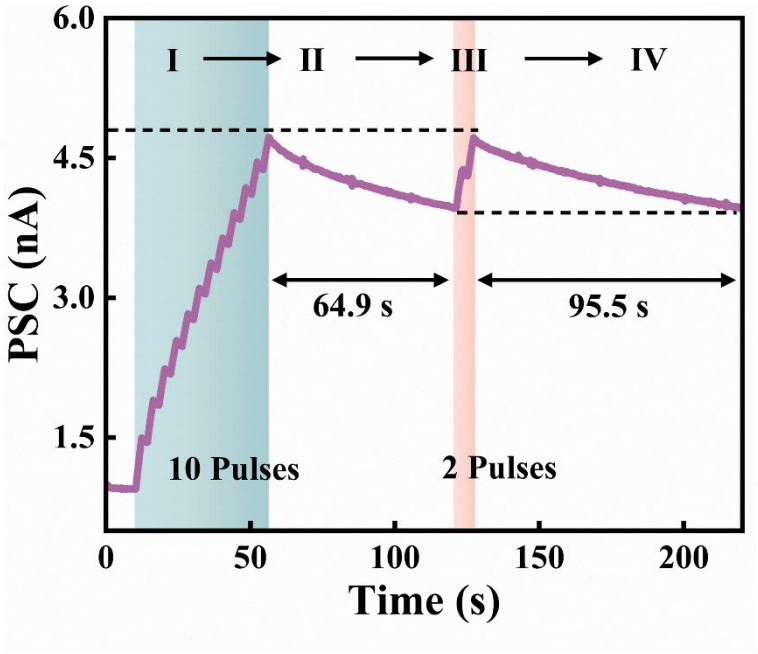

Fig. S8 Emulation of learning-experience behavior under 340 nm light pulse stimulation (0.16 $mW{\cdot}cm^{-2}$, 2 s).

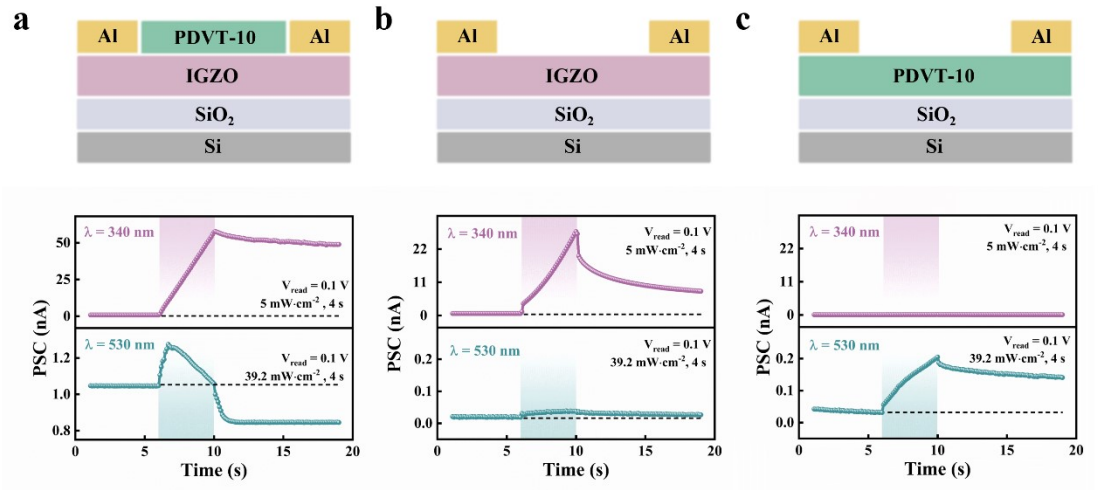

Fig. S9 Photocurrent response of (a) PDVT-10/IGZO heterojunction device, (b) single-layer IGZO device, (c) single-layer PDVT-10 device under 340 nm and 530 nm illumination.

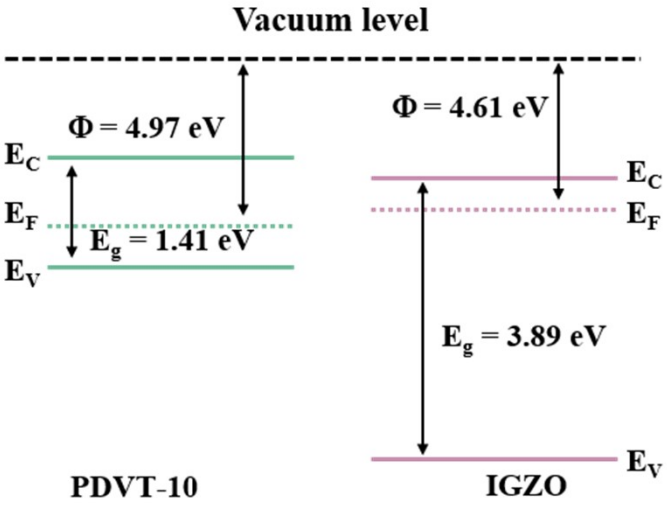

Fig. S10 Energy band structure of IGZO and PDVT-10 films before contact.

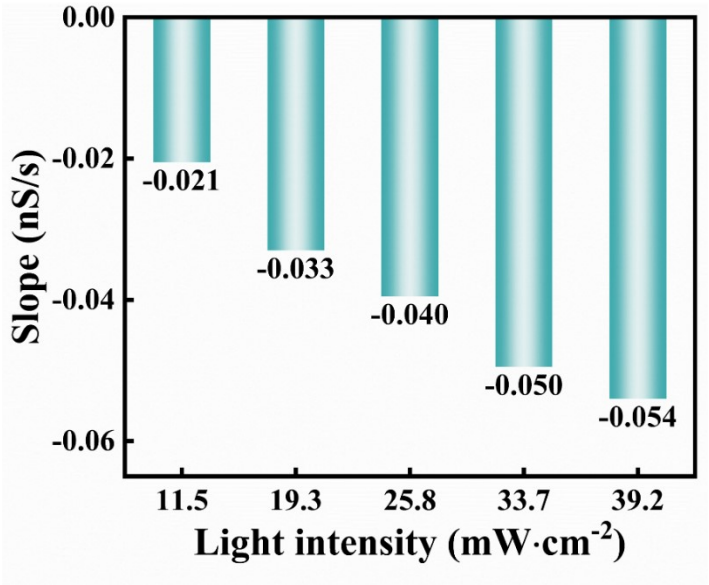

Fig. S11 Decay slope of the photocurrent during 530 nm light illumination, measured under increasing light intensities.

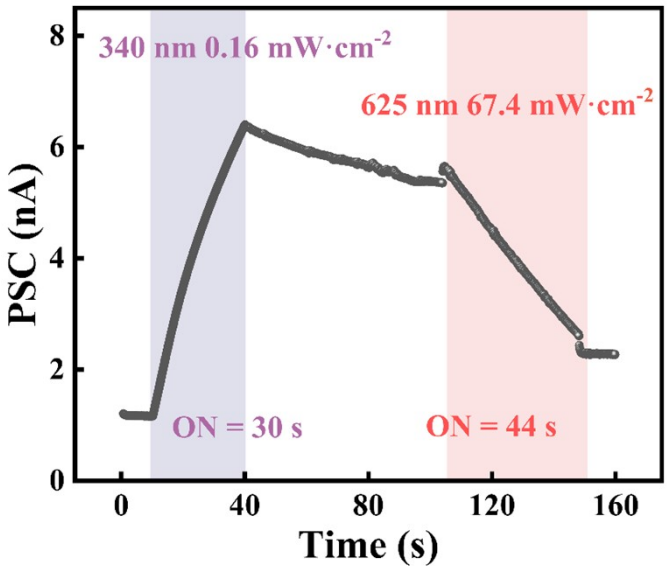

Fig. S12 Reversible photocurrent modulation induced by 340 nm (0.16 mW·cm^{-2}, 30 s) and 625 nm (67.4 mW·cm^{-2}, 44 s) light.

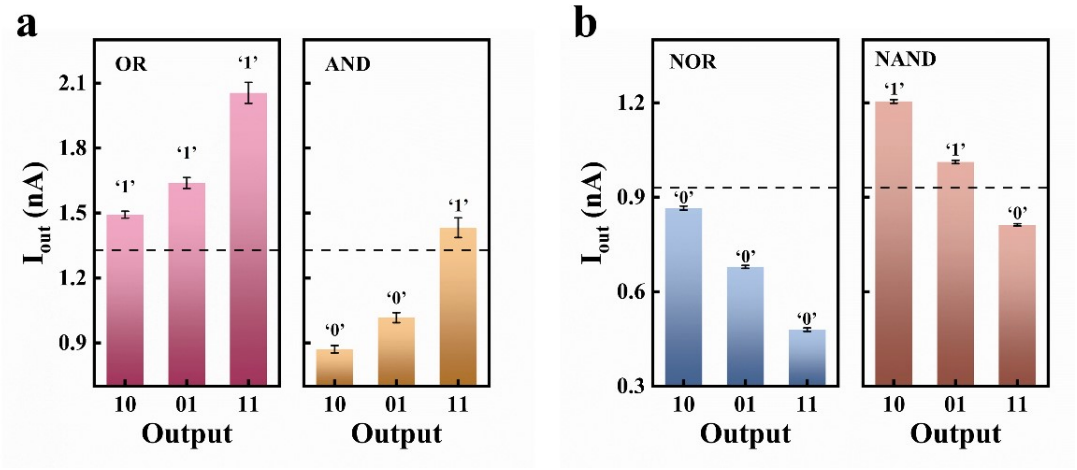

Fig. S13 Reliability of all-optical logic operations. (a) 20 repeated experiments on "OR" and "AND" logic operations performed using two 340 nm optical pulses. (b) 20 repeated experiments on "NOR" and "NAND" logic operations performed using two 530 nm optical pulses.

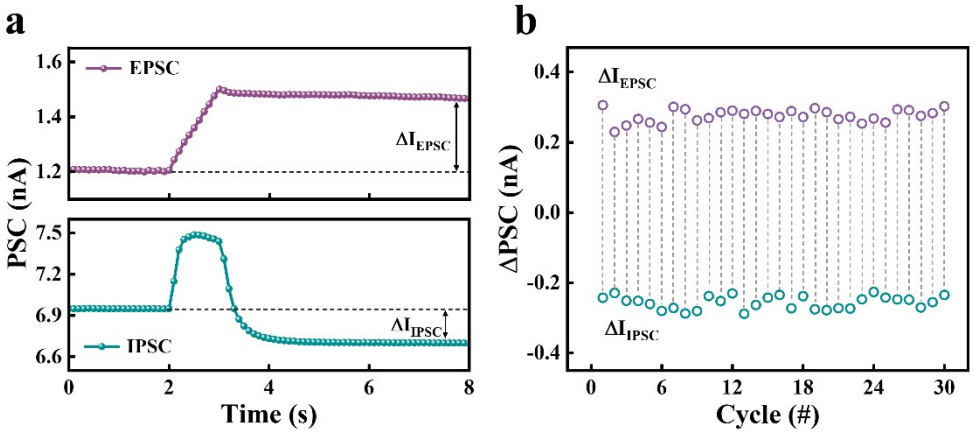

Fig. S14 (a) Photocurrent response curves of a single device under 340 nm (0.16 mW·cm^{-2}, 1 s) and 530 nm (39.2 mW·cm^{-2}, 1 s) light pulse stimulation. (b) 30 cycles of photocurrent changes (ΔI_{EPSC} and ΔI_{IPSC}).

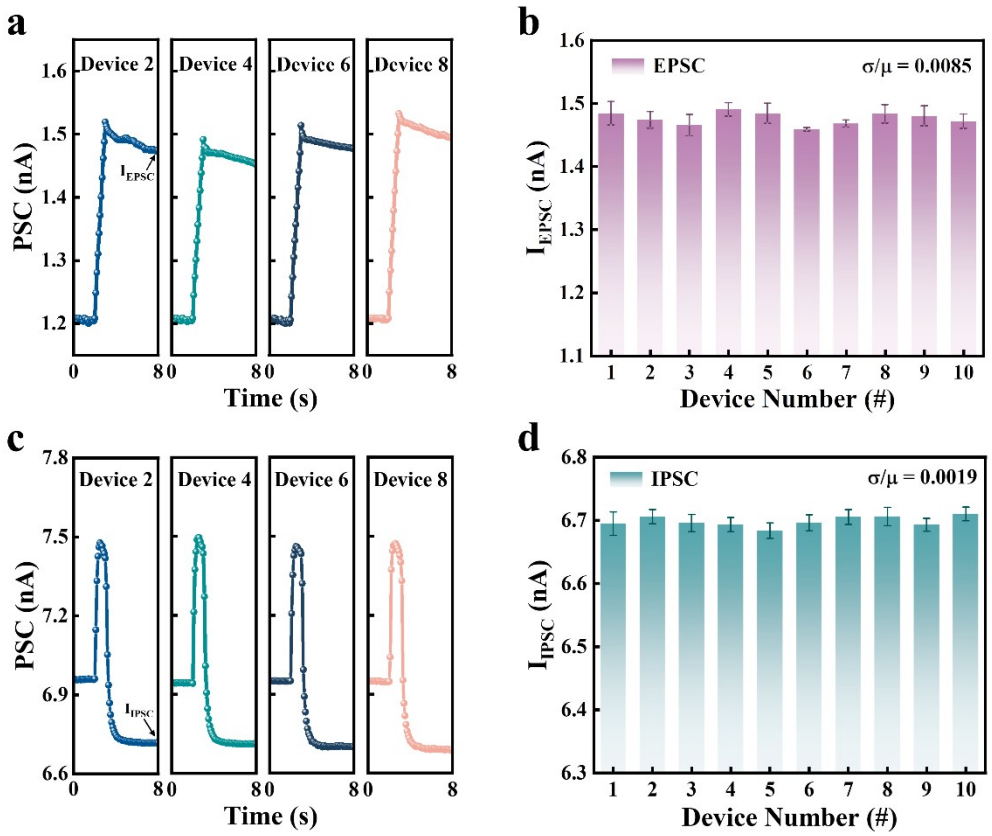

Fig. S15 (a) Photocurrent response curves of ten different devices under 340 nm (0.16 mW·cm^{-2}, 1 s) and 530 nm (39.2 mW·cm^{-2}, 1 s) illumination, respectively. (b, d) Statistical distributions of steady-state photocurrent values (I_{EPSC} and I_{IPSC}) extracted from ten different devices, with the coefficients of variation (σ/μ) of 0.0085 and 0.0019 for I_{EPSC} and I_{IPSC}, respectively.

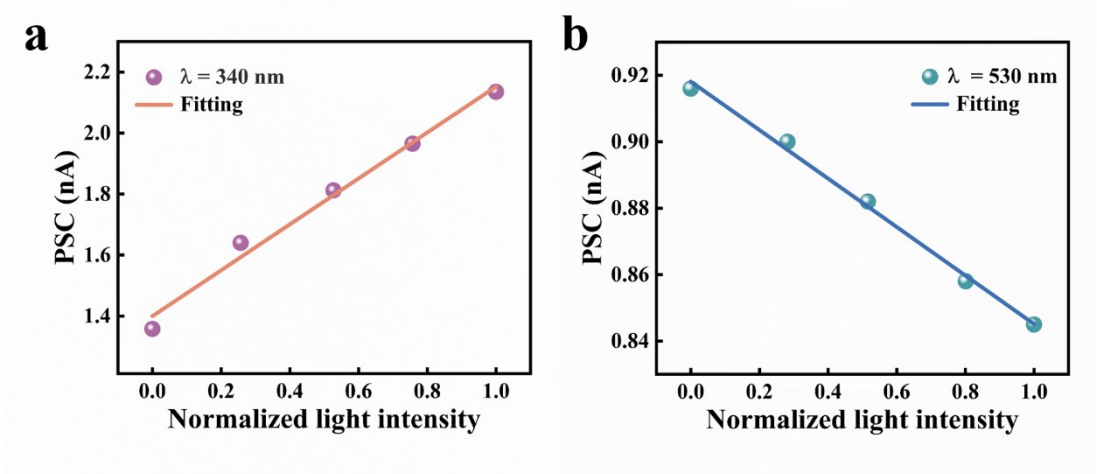

Fig. S16 Relationship between normalized light intensity and PSC of the AOM device (a) under 340 nm illumination, (b) under 530 nm illumination.

Table S1. Four logic functions truth table and corresponding output currents for the synaptic device.

Logic Gate	Input A	Input B	Output Current (nA)	Output Logic
OR	0	0	1.20	0
	1	0	1.48	1
	0	1	1.62	1
	1	1	2.00	1
AND	0	0	0.59	0
	1	0	0.87	0
	0	1	1.02	0
	1	1	1.43	1
NOR	0	0	1.04	1
	1	0	0.87	0
	0	1	0.68	0
	1	1	0.48	0
NAND	0	0	1.37	1
	1	0	1.20	1
	0	1	1.01	1
	1	1	0.81	0

Table S2. Comparison with previously reported AOM artificial synapses with our IGZO/PDVT-10

heterojunction synaptic device.

Device structure	Operation wavelength (nm)		Operation voltage (V)	Light-tuned ratio	Air stability	Endurance (Cycles)	ANN		Ref
	Potentiation	Depression					Epochs	Accuracy [a)]	
Graphene/C_{60}/PbPc	980	405-850	-10 - -50 (V_G)	-	-	-	-	-	[3]
IDTBT/ITO	450	450	20 (V_G)	-	-	-	-	-	[4]
α-In_2Se_3	450, 520, 675	450, 520, 675	10 (V_G)	-	-	18	40	97%	[5]
RP PVK /AlGaN/GaN	457, 532, 660	457, 532, 660	-6 (V_G)	-	-	-	-	-	[6]
Graphene/Ge	1550	1550	3 (V_G)	-	-	-	-	-	[7]
Ga_2O_3/WSe_2	254	520	10/15 (read voltage)	-	-	-	-	-	[8]
ZnSiSnO/ SnO	635	400	5 (read voltage)	≈ 1.56	-	70	50	93.7%	[9]
$PtSe_{2-x}$	980	405	1 (read voltage)	-	-	-	-	-	[10]
ZnAlSnO/ SnO	635	532	0.1 (read voltage)	3.79	4 months	50	30	92.74%	[11]
PDVT-10/ IGZO	340	530	0.1 (read voltage)	8.2	9 months	20	20	97.4%	This work

[a)] "Accuracy" refers to the recognition accuracy of artificial neural networks (ANNs) for handwritten digits from the Modified National Institute of Standards and Technology (MNIST) dataset.

REFRENCES

1. H. Xu, L. Zou, J. An and S. Lin, *ACS Omega*, 2025, **10**, 16884-16891.
2. T. Zhang, C. Fan, L. Hu, F. Zhuge, X. Pan and Z. Ye, *ACS Nano*, 2024, **18**, 16236-16247.
3. Q. Dai, G. Hu, W. Lv, S. Xu, L. Sun, G. F. Schneider, L. Jiang and Y. Peng, *Adv. Mater.* Interfaces, 2022, **9**, 2200116.
4. C. Liu, C. Gao, W. Huang, M. Lian, C. Xu, H. Chen, T. Guo and W. Hu, *Sci. China-Mater.*, 2024, **67**, 1500-1508.
5. Y. Chen, M. Zhang, D. Li, Y. Tang, H. Ren, J. Li, K. Liang, Y. Wang, L. Wen, W. Li, W. Kong, S. Liu, H. Wang, D. Wang and B. Zhu, *ACS Nano*, 2023, **17**, 12499-12509.
6. X. Hong, Y. Huang, Q. Tian, S. Zhang, C. Liu, L. Wang, K. Zhang, J. Sun, L. Liao and X. Zou, *Adv. Sci.*, 2022, **9**, 2202019.
7. J. Fu, C. Nie, F. Sun, G. Li, H. Shi and X. Wei, *Sci. Adv.*, 2024, **10**, eadk8199.
8. Y. Zou, Y. Liu, X. Zhao, Y. Wang, Y. Xin, H. Zhan, X. Feng, S. Yu, W. Ding, Z. Fu, X. Hou and S. Long, *ACS Nano*, 2025, **19**, 30823-30832.
9. Q. Chen, R. Yang, D. Hu, H. Lin, J. Shi, Z. Ye, D. Chen and J. Lu, *Mater. Today*, 2025, **89**, 107-117.
10. Y. Lian, J. Han, M. Yang, S. Peng, C. Zhang, C. Han, X. Zhang, X. Liu, H. Zhou, Y. Wang, C. Lan, J. Gou, Y. Jiang, Y. Liao, H. Yu and J. Wang, *Adv. Funct. Mater.*, 2022, **32**, 2205709.
11. R. Yang, Y. Wang, S. Li, D. Hu, Q. Chen, F. Zhuge, Z. Ye, X. Pi and J. Lu, *Adv. Funct. Mater.*, 2024, **34**, 2312444.